Journal of New Materials for Electrochemical Systems 17, 133-138 (2014)

Carbon Supported Au-Pd-PdO with Low Metal Loading for Electro-oxidation of Methanol in Alkaline Medium

V-H Ramos-Sánchez[1], Diana Brito-Picciotto[2], Ramón Gómez-Vargas[3], David Chávez-Flores[1] and Edgar Valenzuela[4,*]

[1]Facultad de Ciencias Químicas, Universidad Autónoma de Chihuahua,
Nuevo Campus Universitario, Circuito Universitario, Chihuahua, Chih., México. C.P. 31125
[2]Unidad de Energía Renovable, Centro de Investigación Científica de Yucatán,
A.C., Calle 43 #130, Col. Chuburná de Hidalgo, Mérida Yuc., México. C.P. 97200
[3]Energías Renovables y Protección del Medio Ambiente, Centro de Investigación en Materiales Avanzados,
S.C., Miguel de Cervantes #120, Complejo Industrial Chihuahua, Chihuahua, Chih., México. C.P. 31109
[4]Facultad de Ingeniería, Universidad Autónoma de Baja California,
Campus Mexicali, Boulevard Benito Juárez S/N, Mexicali, B. C., México. C.P. 21900

Received: March 20, 2014, Accepted: August 15, 2014, Available online: October 03, 2014

Abstract: *The present work examined two Pd-based alloys supported on carbon: AuPd and Au_2Pd, both synthesized by chemical reduction with $NaBH_4$. The low Au-Pd loading electrocatalysts were physicochemically and electrochemically characterized. Electrocatalytic activity for methanol oxidation was found exclusively in AuPd/C. However, it was revealed that such reaction was promoted by PdO occurring in the actual active phase of the supported electrocatalyst, through the formation of Au-Pd-PdO ensemble sites.*

Keywords: Au-Pd nanoparticles, bimetallic alloy, alkaline direct alcohol fuel cell, methanol electro-oxidation.

1. INTRODUCTION

Alkaline direct alcohol fuel cells, ADAFC, can be considered a hybrid technology. These result from alkaline fuel cells (AFC) and direct alcohol fuel cells (DAFC). ADAFC have attracted much attention recently, because these have overcome many of the major issues encountered in AFC and DAFC. As a matter of fact, the exploitation of alkaline anion exchange membranes (AAEM) as electrolytes in ADAFC brings with it inherent benefits, such as carbonation prevention and reduced alcohol crossover. Added to that, an alkaline regime eases both alcohol oxidation and oxygen reduction [1, 2].

Platinum (Pt), either in acid or basic media, has shown the best catalytic activity for methanol electro-oxidation. Therefore, Pt and Pt-based electrocatalysts have been traditionally used in direct methanol fuel cells (DMFC) [3]. However, the high price and limited supply of Pt make it prohibitive for large scale production.

Alkaline direct methanol fuel cells (ADMFC) exhibit weak specific adsorption of spectator ions in basic media and high coverage of adsorbed OH at low potential, necessary for methanol electro-oxidation. These two characteristics even permit superior catalytic performance of other noble metals in addition to Pt, according to the following reactions:

$$CH_3OH+6OH^- \rightarrow CO_2+5H_2O+6\bar{e} \quad \left[E_a^o = 0.81\text{V}\right] \quad (1)$$

$$\tfrac{3}{2}O_2+3H_2O+6\bar{e} \rightarrow 6OH^- \quad \left[E_c^o = 0.40\text{V}\right] \quad (2)$$

For instance, in alkaline media, Pd nanoparticles have demonstrated higher catalytic activity than those of Pt for ethanol electro-oxidation; a quite opposite performance has been found in methanol electro-oxidation under the same conditions [4]. Based on this statement, Pd on its own should not be considered a suitable electrocatalyst particularly for ADMFC; nonetheless Pd-based electrocatalysts should not be discarded under these terms. In fact, Pd-based bimetallic nanoparticles besides being an option to over-

*To whom correspondence should be addressed:
Email: evalenzuela.mondaca@uabc.edu.mx

come the limited supply of Pt for large scale production of fuel cells electrocatalysts, they are also an alternative to further explore methanol electro-oxidation in alkaline media. Note that the importance of methanol as a fuel relies on the fact that is the alcohol with the shortest carbon chain, which make it the most efficient hydrogen carrier, among the alcohols. No other alcohol is capable to emit less CO_2 during fuel cell operation.

In the particular case of AuPd nanoparticles, there is an outstanding synergistic effect when Pd is combined with gold (Au), since the latter favors the stability of the former, preventing thus Pd dissolution in highly oxidizing conditions [5] and acts as an electronic promoter for Pd, almost certainly due to its strong capacity to withdraw electrons. Another important effect of Au over Pd is the weakening of its binding strength, which avoid strong interactions between adsorbates (*e.g.* CO) and Pd active surface area [6]. Thus, in virtue of the aforesaid enhancement, the acceptance of using Au, a precious metal twice more expensive than Pd [7], in supported catalysts is such that since 1960s, the catalytic properties of Au-Pd have been investigated, mainly for hydrocarbon processing [8]. To date, AuPd electrocatalysts are still being investigated for methanol electro-oxidation and high activity has been reported through novel fabrication procedures [9, 10].

Overall, among the key factors that affect the activity of bimetallic electrocatalysts during electrooxidation in an ADAFC are the components arrangement (alloy, heterostructure and core-shell), surface structure, particle size, and alloying degree. At this last point, the electrocatalyst synthesis route plays an important role in controlling metal deposition and ultimately the alloying degree in bimetallic particles. Indeed, incomplete alloying of Au-Pd can be originated due to a faster reduction of Au, when employing sodium borohydride ($NaBH_4$), particularly if both electrocatalyst precursors are dissolved in tandem [8]. Thus, if the aforesaid occurs, it is expected to encounter both Au and Au-Pd particles, rather than isolated Pd particles; such chemical behavior, it is understood in terms of the redox potentials of Au (1.00 V) and Pd (0.62 V), which do not allow a galvanic reaction to occur for the electrodeposition of Pd, through the reduction of the $PdCl_4^{2-}$ ion, on the surface of Au.

It has also been found a positive effect of PdO over Pd-based catalysts, where in some cases it is necessary their coexistence to get highly active catalysts [11]. As a matter of fact, there is an optimum Pd:PdO ratio to achieve optimum catalytic activity [12]. There are also suggestions of the existence of two different types of PdO, one with high catalytic activity; and another with poor catalytic performance. The former has been associated with moderate temperature and the latter with high temperature [13].

In this context, the present paper is concerned with the synthesis and characterization of a low metal loading electrocatalyst: Au-Pd/C. Data from two different carbon supported alloys, AuPd and Au_2Pd, is discussed. The comparison of these two systems was chosen to emulate a scenario wherein palladium has been partially depleted due to its unavoidable dissolution during continuous operation of an ADMFC.

2. EXPERIMENTAL DETAILS

2.1. Preparation of Au-Pd/C Electrocatalysts

Carbon-supported AuPd nanoparticles with two different compositions [2:1] and [1:1], Au_2Pd and AuPd hereinafter, were synthesized by simultaneous chemical reduction of $HAuCl_4$ and Na_2PdCl_4 in presence of $NaBH_4$ as a reducing agent.

The Au_2Pd and AuPd nanoalloys were prepared by dissolving appropriate amounts of $HAuCl_4$ and Na_2PdCl_4 in 50 mL of deionized water, as summarized in table 1. The two resulting aqueous solutions were then heated at 50°C under air atmosphere. In tandem, a protective agent was obtained by dissolving 300 mg of Polyvinylpyrrolidone (PVP40) in 100 mL of methanol. Afterwards, each of the two aqueous solutions containing the precursors were mixed, separately, with 50 mL of the solution containing PVP40 and kept under stirring under air atmosphere. These metallic admixtures were then chemically reduced by the drop-wise incorporation of 6 mL of a 66 mM $NaBH_4$ solution. All reagents were high purity, 99.99% or better, from Sigma Aldrich, except for $NaBH_4$ which was obtained from Fluka.

The aforesaid procedure yielded two colloidal dispersions, AuPd and Au_2Pd. In order to obtain either of the supported bimetallic electrocatalysts, AuPd/C or Au_2Pd/C, 1 g of carbon black (Vulcan XC72) was oxidized with 500 mL of H_2O_2 (30wt%) at 40°C, and just before the carbon paste got dry, 1 mL of the corresponding colloidal dispersion was added, later, when the powder was dry, it was copiously rinsed with deionized water and then treated at 330°C in air for 20 minutes to promote alloy formation and to remove impurities at the catalyst surface.

2.2. Characterization Methods

X-ray diffraction (XRD) was carried out directly on the supported electrocatalysts using a Siemens D5000 diffractometer with a step of 0.1° from 5° to 90° 2θ, 5s/step; and employing a Cu Kα radiation´s wavelength of 1.541877 Å. Thermogravimetric analysis (TGA) was performed within a TGA Q500 from TA Instruments. The sample (*ca.* 20 mg) was heated in a platinum pan from room temperature up to 950°C at a temperature slope of 10°C/min under air atmosphere. X-ray fluorescence (XRF) measurements were made in a Horiba XGT-1000WR spectrometer equipped with a Rh X-ray source and a high purity Si detector. A Jeol 100 CX was used for transmission electron microscopy (TEM) analysis of the bimetallic particles. For this purpose, a drop of each of the nanoparticle colloidal dispersions was placed separately on a copper grid and later dried for its observation under the microscope.

2.3. Electrochemical Measurements

Electrochemical characterization of the supported electrocatalysts was conducted at room temperature (20 ± 0.5°C) in a three-electrode glass cell consisting of a platinum rod as counter electrode; a saturated calomel electrode (SCE) serving as reference, which was contained in a Luggin capillary to prevent any contamination; and carbon paper with an area of 1 cm^2 acting as working electrode. The reference electrode was fixed close to the working electrode through a Luggin capillary. The working electrode was produced by dropping a suitable amount of alcoholic sol containing the electrocatalyst onto the carbon paper; such sol was prepared

Table 1. The amounts of precursors weighed and expected compositions of AuPd particles.

Sample	System	mmol Au	mmol Pd	mg $HAuCl_4$	mg Na_2PdCl_4
Au_2Pd	[2:1]	0.99	0.33	33.63	9.70
AuPd	[1:1]	0.66	0.66	22.42	19.41

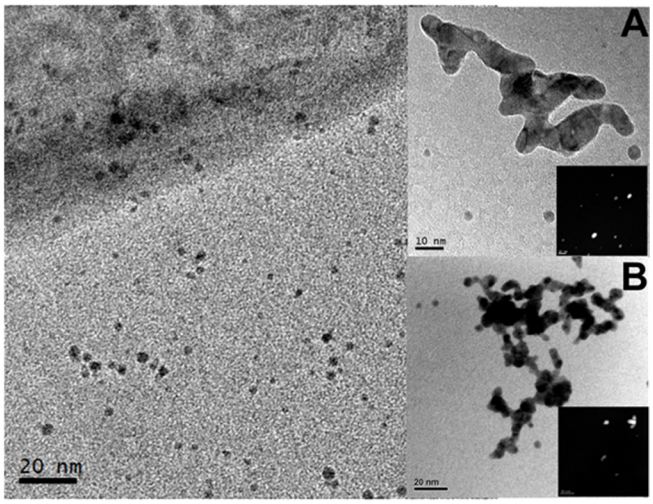

Figure 1. TEM images of the colloidal dispersions of: A) Au_2Pd; and B) AuPd. Inset in each figure displays a HAADF-STEM micrograph of its corresponding system.

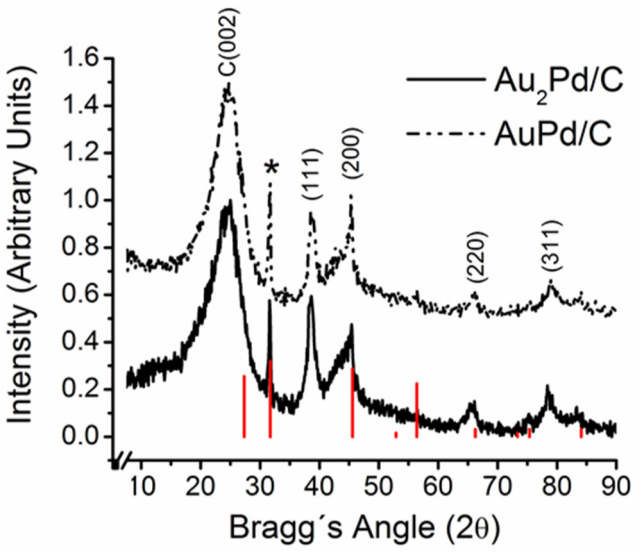

Figure 2. X-ray diffractograms of the bimetallic supported electrocatalysts with the indexed planes of PdO represented as red sticks.

dispersing ultrasonically 20 mg of the carbon supported electrocatalyst in 0.5 mL of isopropanol to which 25 μL of 5wt% Nafion solution were added, during 20 minutes.

Cyclic voltammetry (CV) and electrochemical impedance (EIS) measurements were performed in 0.5 M NaOH in absence and presence of 1 M methanol, using a Voltalab Potentiostat/Galvanostat model PGZ 301. In both experimental scenarios, the electrolyte (0.5 M NaOH) was bubbled with high purity nitrogen gas for deaeration during one hour before initiating any electrochemical analysis. Whereas voltammogram curves were acquired at 50, 25 and 10 mV/s; impedance spectra were recorded at open circuit potential (-173 mV for AuPd and -204 mV for Au_2Pd *vs* SCE) in a frequency range between 100 kHz to 10 mHz and an amplitude AC signal of 10 mV.

3. RESULTS AND DISCUSSION

3.1. Electrocatalyst Characterization

Figure 1 shows the micrographs of the Au_2Pd and AuPd colloidal dispersions. The size of the metallic particles was found in a range between 2 and 5 nm. A qualitative interpretation of TEM analysis performed on a couple of TEM micrographs showing irregular agglomeration of metal particles (insets in fig. 1A and 1B) obtained from high angle annular dark field scanning transmission electron microscopy (Z-contrast) revealed that there was not just one single phase occurring in the colloidal dispersions; which is likely to result of an incomplete alloying process between Au and Pd during simultaneous chemical reduction. This observation made evident that a high temperature treatment during particles support is compulsory, in order to complete alloy formation. All of the above derived from the fact that under Z-contrast conditions, the micrographs exhibited several dots within the specimens in which the brightness was not similar.

To verify the alloying degree in both supported bimetallic systems, XRD and XRF were exploited. Figure 2 displays the XRD patterns of Au_2Pd/C and AuPd/C. In both cases, the diffractograms revealed peaks that relate to the (111), (200), (220) and (311) planes indexed for Au (JCPDS 04-0784) and Pd (JCPDS 05-0681) in their face centered cubic structures. Although all of these XRD features observed in the diffractograms result of the sum of two single diffraction peaks, it was remarkable to identify a reflection for tetragonal PdO, evolving from the convolution of its facets (002) and (101); such observation made clear that peak *ca.* 45º should also include a significant contribution from the (110) plane of PdO (JCPDS 75-0584), as illustrated by red sticks representing the indexed peaks of PdO. With respect to the carbonaceous electrocatalyst support, the diffractograms allowed to identify unequivocally a broad band *ca.* 25º, attributed to the (002) plane of turbostratic carbon, which is clearly evident in both XRD patterns. Isolated reflections for Au-Pd (alloy) and PdO, *ca.* 39º and 32º respectively, were chosen to estimate the mean crystallite size according to the Debye-Scherrer equation. Peak fitting analysis correspondingly indicated crystallite sizes of about 5 nm and 19 nm for Au-Pd and PdO. Also using the results of the peak fitting analysis of the XRD patterns, the alloying degree in both electrocatalysts was calculated using Vegard's law, based particularly on the position of the (111) peak for Au-Pd; since that is one of the two Au-Pd reflections free of contribution from PdO. According to the above,

Table 2. Summary of relevant characterization results of the supported catalysts.

Sample	Composition		Components	Crystallite sizes (nm)		Metal loading
	Alloy	Atomic		Au-Pd	PdO	
Au_2Pd/C	$Au_{0.77}Pd_{0.23}$	$Au_{0.67}Pd_{0.33}$	Au-Pd, PdO; H_2O; C	4.8	16.9	3.5%
AuPd/C	$Au_{0.64}Pd_{0.36}$	$Au_{0.48}Pd_{0.52}$	Au-Pd; PdO; C	5.6	21.6	4.0%

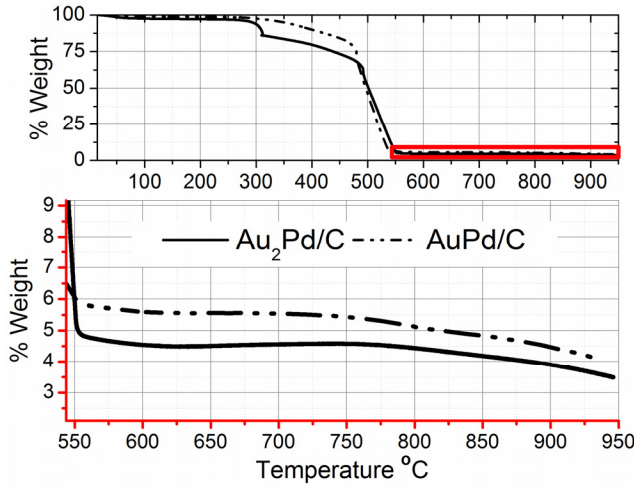

Figure 3. *Top*: Thermograms of Au_2Pd/C and AuPd/C. *Bottom*: Zoom in on the PdO decomposition region.

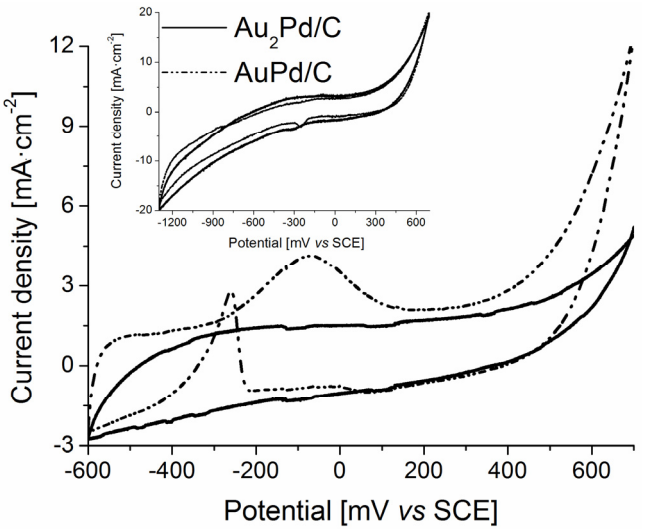

Figure 4. Cyclic voltammograms of methanol electrooxidation on the Au-Pd electrodes in 0.5 M NaOH solution containing 1.0 M methanol with a scan rate of 10 mV/s. *Inset*: Cyclic voltammograms of hydroxyl (OH^-) adsorption/desorption in 0.5 M NaOH solution at 10 mV/s.

the atomic percent of alloying Au in Au_2Pd/C was 77% and 64% in AuPd/C. These values were, however, in discrepancy with the XRF atomic compositions, as shown in table 2. The difference among atomic compositions yields that 33% and 50% of the Pd within Au_2Pd/C and AuPd/C, respectively, is in the form of PdO.

In order to determine the metal loadings of the two supported electrocatalysts TGA was exploited. Figure 3 presents the analytical thermograms of Au_2Pd/C and AuPd/C. Several insights were inferred through simple observation. In the case of Au_2Pd/C, it is evident an early weight loss that stabilizes around 100°C that, accordingly, it has been associated with water evaporation. Another drop, *ca.* 300°C, solely observed in Au_2Pd/C was attributed to a partial reduction of PdO according to reaction 3, which releases oxygen. Then, PdO decomposition is only evident in Au_2Pd/C, since it has been found that such reaction is benefitted as Au:Pd molar ratio increases in the alloy [14].

$$2x\mathrm{Au} + 2\mathrm{PdO} \rightarrow 2\mathrm{Au}_x\mathrm{Pd} + \mathrm{O}_2 \quad (3)$$

Then, a uniform behavior was observed for both electrocatalysts, where full thermal decomposition of the carbonaceous support was achieved at 550°C; followed by the melting and ultimate conversion of PdO to Pd starting at 750°C [15]. Thus, based on the analytical thermograms, the actual metal loadings in Au_2Pd/C and AuPd/C were 3.5% and 4.0%, respectively.

3.2. Electrochemical Performance

The cyclic voltammograms for the Au_2Pd/C and AuPd/C in alkaline media are shown in figure 4. Whereas, the main plot in figure 4 is intended to observe methanol electrooxidation; the inset within should display the characteristic hydroxyl (OH^-) adsorption/desorption process.

Although similar, both voltammograms presented in the inset in figure 4 revealed two distinct cathodic peaks *ca.* -300 mV, which were attributed to the reduction of PdO (reaction 4) already present in both electrocatalysts, as previously demonstrated. It is noteworthy that no clear evidence of sorption processes was found. Even though, the electrochemically active surface area (ECSA) was calculated for AuPd/C (434.9 cm^2/mg) based on the PdO reduction peak; subsequently the electrocatalytic activity was only qualitatively assessed due to the significant uncertainty derived of the occurrence of PdO in the original composition of both electrocatalysts and therefore the abovementioned value for ECSA of AuPd/C should be taken with caution.

$$\mathrm{PdO} + \mathrm{H_2O} + \bar{e} \rightarrow \mathrm{Pd} + 2\mathrm{OH}^- \quad (4)$$

At this point, and despite the lack of adsorption and desorption peaks; it was outstanding to observe in figure 4, only for AuPd/C, the capability of promoting electrooxidation of methanol in alkaline media, even if it is at a higher onset potential (-437 mV) with respect to Pd/C (-590 mV) [16]. Methanol oxidation in alkaline media has been characterized by two anodic peaks obtained during the forward and reverse scan. The former is usually related to the oxidation of freshly chemisorbed species from methanol adsorption; whereas the latter is fundamentally associated to removal of the carbonaceous species originated during the aforesaid chemisorption process [16]. Therefore, it was suffice to observe just one of these anodic peaks to verify the electrocatalytic activity of AuPd/C. Finishing with a detailed description of the cyclic voltammogram of methanol oxidation on the surface of AuPd/C, there is a broad anodic peak centered at -75 mV caused by the formation of an oxide of the alloy. The complementary cathodic peak corresponding to the reduction of the oxide of the alloy is diffuse, and roughly centered at 70 mV.

The impedance results are shown in figure 5. The EIS experimental data was simulated using ZPLOT software. The values obtained for the Charge Transfer Resistances (R_{CT}) and Constant

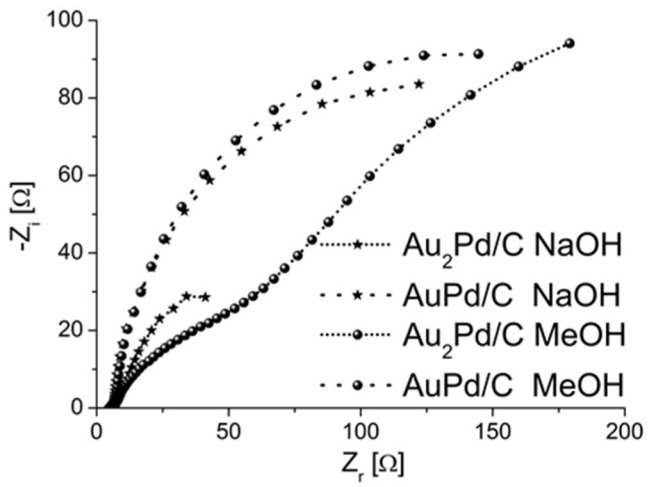

Figure 5. Nyquist plots of the EIS results obtained for Au_2Pd/C and AuPd/C in alkaline media, in presence or absence of methanol. The experimental data is represented by stars and spheres; simulations are presented as dotted lines.

Phase Elements (CPE) are summarized in table 3, and the electric equivalent circuits used for the simulation are presented in figure 6. Whereas, CV offered an insight to particular processes; EIS was addressed to study the overall behavior of the electrocatalyst at the electrode/electrolyte interface.

In both materials, a response controlled by a Faradaic process was observed. For the AuPd/C sample, the Nyquist diagrams in presence and absence of methanol were represented with a single semicircle slightly depressed. This response is typical for an electrode/electrolyte interface, where the charge transference between the electrocatalyst and the chemical species in the electrolyte is accomplished in one single step [17]. This behavior is highly desirable in an electrocatalyst, since as the number of steps involved in the oxidation/reduction of species diminishes, the overall kinetics of the process is increased.

A complete different scenario was observed in the Au_2Pd/C sample where two overlapped semicircles were obtained. This response is attributed to two different processes associated to an additional interface comparable to the AuPd/C system. At this point it is worth to recall the analytical thermogram of Au_2Pd/C in figure 3, which shows an evident PdO decomposition at about 300°C. This means that according to the heat treatment used during synthesis, a significant amount of PdO in Au_2Pd/C should be reduced by isolated Au. In this context, a feasible explanation to such behavior could be related to Au-Pd-PdO ensemble sites [11]. Hence, in

Table 3. Electrical elements and their values employed during simulations of the electrochemical data.

Sample	MeOH	R_{CT1} (Ω)	CPE_1 (F)	n	R_{CT2} (Ω)	CPE_2 (F)	n
Au_2Pd/C	(+)	109.60	0.0074	0.52	245	0.039	0.80
Au_2Pd/C	(-)	6	0.04	0.70	80	0.15	0.87
AuPd/C	(-)	200	0.057	0.87			
AuPd/C	(+)	220	0.042	0.87			

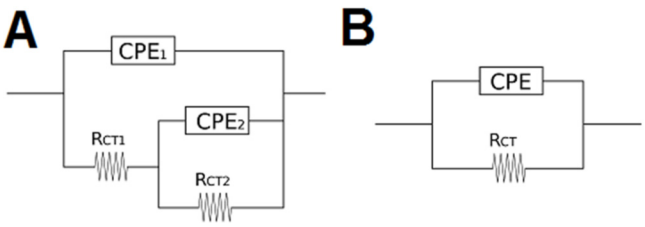

Figure 6. Electrical equivalent circuits used during simulations of the EIS results. A) Au_2Pd/C; and B) AuPd/C.

Au_2Pd/C the PdO available is isolated, such scenario will recreate the two interfaces shown by the two semicircles present solely in Au_2Pd/C impedances, where PdO is the additional interface providing an additional opposition to the charge transference between the chemical species and the electrocatalyst.

When analyzing the Rct values, an interesting behavior is observed. According to the Rct obtained by the Electrical Equivalent Circuits the Au_2Pd + NaOH systems exhibit a lower Rct compared with the same system after the methanol addition. This can be explained considering the low catalytic activity shown by the Au_2Pd material. Under this condition, the methanol is adsorbed in the surface displacing the NaOH charged species and since nil or very low methanol oxidation is occurring, the interface exhibits higher opposition to charge transference when comparing with the values obtained before methanol addition. On the other hand, no matter the same methanol-NaOH replacement is taking place in the AuPd electrode, only a slight increment of the Rct is observed, because the NaOH species displacement is compensated by the increased reactivity towards the methanol oxidation reaction. This observation is in agreement with the cyclic voltammetry analysis that shows a higher catalytic activity of AuPd/C with respect to Au_2Pd/C.

4. CONCLUSIONS

Characterization of Au_2Pd/C and AuPd/C, prepared by co-reduction in aqueous solution, revealed an incomplete alloying and presence of PdO in both systems. AuPd/C demonstrated electrocatalytic activity to promote methanol oxidation in alkaline media, at higher potentials than Pd/C on its own. In fact, cyclic voltammetry put forward that nanostructured PdO contributes to the active phase in AuPd/C, through the formation of Au-Pd-PdO ensemble sites. In the case of Au_2Pd/C, the PdO at the system is isolated and therefore neither the alloy nor the PdO are capable to promote electrocatalytic activity. Also, there was an implicit suggestion that the deficiency of palladium in Au_2Pd/C could be associated to a preferential reaction pathway, in which the occurrence of PdH_x is benefited over the reduction reaction, and ultimately the alloying process.

5. ACKNOWLEDGEMENTS

This research was funded by the Public Education Ministry (SEP, México) through the PROMEP program under the grant PROMEP/103.5/12/3923.

REFERENCES

[1] F. Bidault, Journal of Power Sources, 187, 39 (2009).
[2] A.V. Tripković, Electrochimica Acta, 47, 3707 (2002).
[3] E. Antolini, E.R. Gonzalez, Journal of Power Sources, 195, 3431 (2010).
[4] C. Xu, Electrochemistry Communications, 9, 997 (2007).
[5] J. Zhang, Science, 315, 220 (2007).
[6] F. Gao, D.W. Goodman, Chemical Society Reviews, 41, 8009 (2012).
[7] U.S. Geological Survey, Report 2012, 204 (2013), http://pubs.usgs.gov/sir/2012/5188.
[8] S.Y. Park, Current Applied Physics, 10, S40 (2010).
[9] J.N. Zheng, Journal of Power Sources, 262, 270 (2014).
[10] X. Wang, Journal of Alloys and Compounds, 565, 120 (2013).
[11] A. Tompos, Combinatorial Chemistry & High Throughput Screening, 10, 71 (2007).
[12] W. Lin, Applied Catalysis B: Environmental, 50, 59 (2004).
[13] G. Groppi, Studies in Surface Science and Catalysis, E. Iglesia, Ed., Elsevier, Amsterdam, (2001), p. 345.
[14] K. Qian, W. Huang, Catalysis Today, 164, 320 (2011).
[15] N.N. Greenwood, A. Earnshaw, Chemistry of the Elements, (1997), Butterworth-Heinemann, Oxford, UK.
[16] S.S. Mahapatra, J. Datta, International Journal of Electrochemistry, Article ID 563495 (2011).
[17] J. Zhang, Electrochimica Acta, 54, 1737 (2009).